Mineralogy of the Nandewar Volcano, northeastern New South Wales, Australia

A. J. STOLZ*

Department of Geology and Geophysics, University of New England, Armidale, NSW, 2351, Australia

ABSTRACT. The paper discusses the mineralogy of eruptives from the Nandewar Volcano, which range in composition from hawaiite and trachyandesite to comendite via tristanite and mafic and peralkaline trachyte. Olivine, Ca-rich pyroxene, and amphibole display marked decreases in 100 Mg/(Mg + Fe) ratios in the sequence trachyandesite to comendite, reflecting variation in host rock compositions. The presence of tschermakitic subcalcic pyroxene and aluminous bronzite megacrysts in several trachyandesites indicates that these experienced intratelluric crystallization at elevated pressures (6-8 kbar). Some titanomagnetite and plagioclase phenocrysts in trachyandesites may also be moderate pressure cognate precipitates. Groundmass pyroxenes of some trachytes and comendites are strongly acmitic. The presence or absence of coexisting alkali amphiboles and aenigmatite appears to reflect stability over a relatively broad range of f_{O_2} conditions. Aenigmatite rims on titanomagnetite and ilmenite microphenocrysts in several peralkaline eruptives provides support for a 'no-oxide' field in T-f_{O_2} space. The Fe–Ti oxide compositional data indicate that magmas spanning the spectrum trachyandesite–comendite crystallized under conditions of decreasing T and f_{O_2} which broadly coincided with the FMQ synthetic buffer curve. However, a voluminous group of slightly older associated rhyolites appear to have crystallized under significantly more oxidizing conditions.

KEYWORDS: olivine, pyroxene, amphibole, feldspar, titanomagnetite, aenigmatite, ilmenite, Nandewar Volcano, New South Wales, Australia.

DETAILED mineralogical studies are important tools in evaluation of the evolution of volcanic suites. This paper discusses the genetic implications of selected mineralogical characters of transitional volcanics comprising the Nandewar Volcano (Abbott, 1969) in northeastern New South Wales, Australia (fig. 1).

The volcanics range in composition from hawaiite and trachyandesite, through tristanite, mafic and peralkaline trachyte to mildly peralkaline (comenditic) and peraluminous rhyolites.

* Present address: Department of Geology, University of Tasmania, Hobart, Tasmania, Australia 7001.

Eruption of a voluminous group of metaluminous to mildly peraluminous rhyolites preceded (by 1-2 Ma, Hensel and Stolz, in prep.) extrusion of the main shield-forming sequence which occurred over the interval 18.0-17.2 Ma (Stipp and McDougall, 1968; Wellman et al., 1969; Wellman and McDougall, 1974). The main shield-forming eruptives, which include hawaiites, trachyandesites, tristanites, and trachytes, were subsequently intruded by dykes and plugs of peralkaline trachyte and comendite. The field relations, petrography, chemistry, and petrogenesis of the Nandewar volcanics are discussed in more detail elsewhere (Stolz, 1985).

Mineralogy

Phases were analysed using a TPD probe at the Research School of Earth Sciences, Australian National University, and a Jeol JSM-35, Tracor–Northern instrument at the University of New England. Operating conditions and correction procedures are outlined by Ware (1981). Where given, Zr and Zn data were determined under similar operating conditions, using the Tracor–Northern multiple-least-squares peak-fitting routine followed by Bence and Albee matrix corrections.

Olivine is common as phenocrysts or microphenocrysts in the hawaiites and trachyandesites, less common in tristanites and trachytes and absent from the rhyolites. Compositions range from Fo_{88} in the trachyandesites to Fo_{10} in the trachytes (Table I). In several peralkaline trachytes fayalitic microphenocrysts are rimmed by clinopyroxene similar in composition to groundmass pyroxenes suggesting that early-crystallizing olivine was in reaction with liquid.

The mg values (100 Mg/(Mg + ΣFe)) of the olivines decrease regularly as functions of host mg over the compositional range trachyandesite to trachyte. Olivine Ca and Mn contents also decrease (fig. 2) and Ni increases with increasing olivine mg. Comparable increases in olivine Ca and Mn contents occur in similar volcanics from Ethiopia
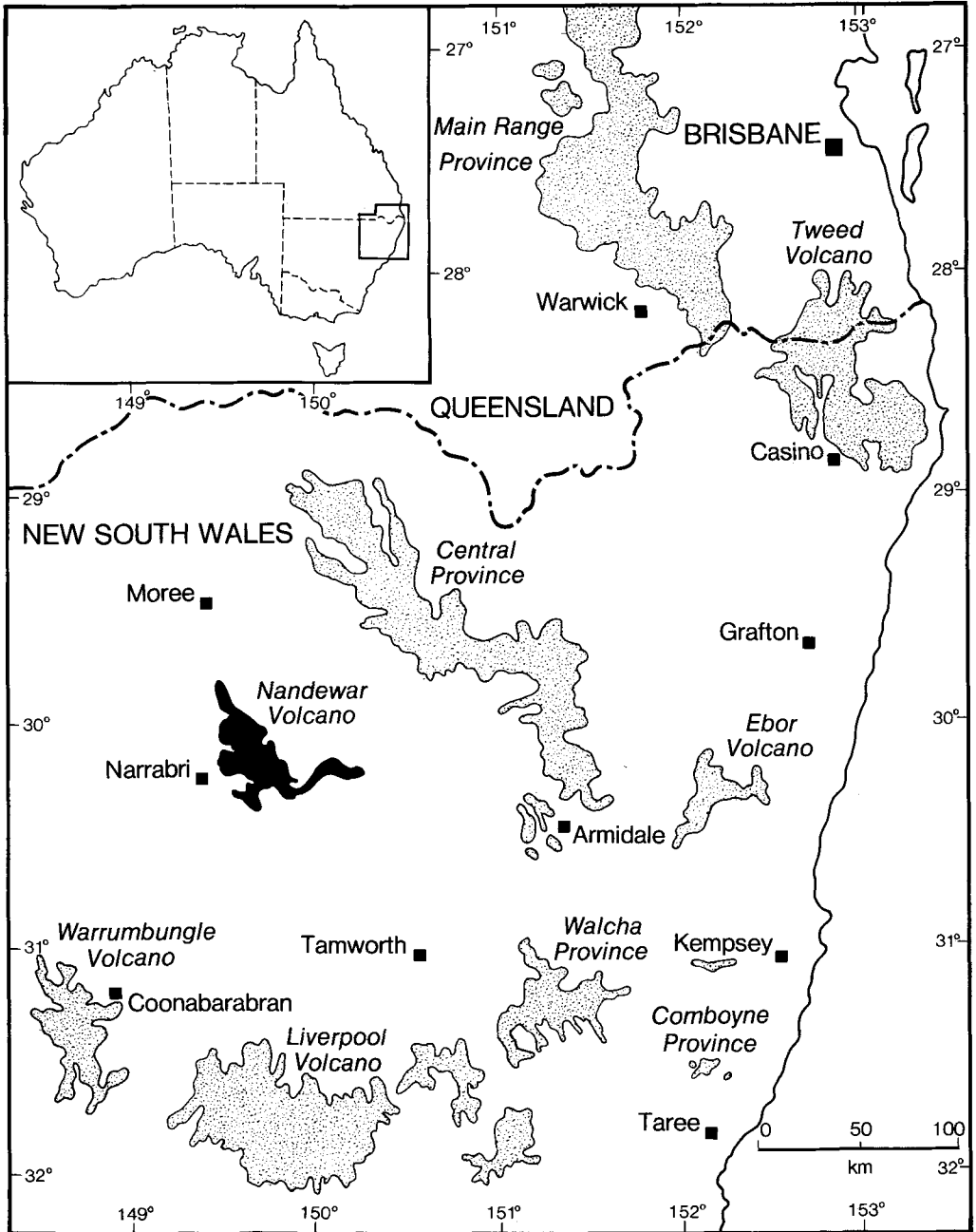
FIG. 1. Location of the Nandewar Volcano in relation to other major Cainozoic volcanic provinces in eastern New South Wales and south-eastern Queensland.
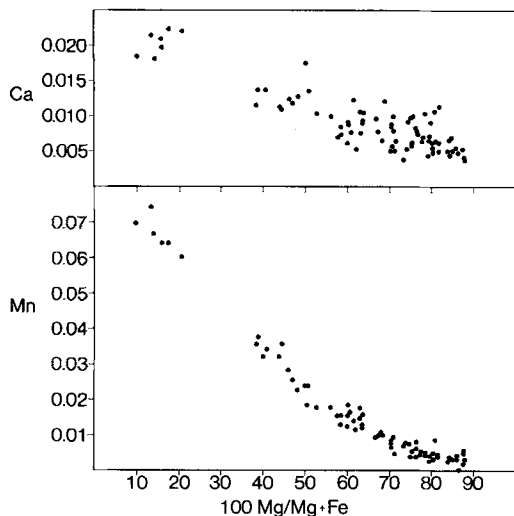
FIG. 2. Variation of Ca and Mn (atoms per formula unit) with *mg* (100 Mg/(Mg + ΣFe)) in olivine.

(Bizouard *et al.*, 1980). The regular increase in the Ca contents of olivines with decreasing *mg* values is not due to either crystallization at decreased pressures (cf. Simkin and Smith, 1970; Stormer, 1973) or Ca content of the melt (Watson, 1979; Wilkinson and Stolz, 1983), but instead is probably a function of increasing SiO_2 and Fe/Mg of the host (Roeder, 1974). Experimental data from several synthetic systems (Takahashi, 1978; Watson, 1979) indicate that partitioning of Mn between olivine and liquid

is dependent on temperature and melt composition, $K_{Mn}^{ol/liq}$ increasing with SiO_2 content of the melt.

Pyroxenes exhibit a broad range of compositions (Table II) and occur in three principal modes: 1. Ca-rich and Ca-poor megacrysts of inferred high-pressure origin; 2. low-pressure Ca-rich pyroxene phenocrysts; 3. groundmass pyroxenes (ranging in composition from Ca-rich to acmitic types). Partially resorbed 'megacrysts' (3–5 mm) of aluminous subcalcic pyroxene and aluminous bronzite (Table II, Nos. 49008 and 49009) which contain rare inclusions of olivine are restricted to the trachyandesites. The very low Cr contents of the Nandewar Ca-poor pyroxene megacrysts (< 0.08 wt. % Cr_2O_3) contrasts with relatively high levels (0·15–0.41 wt. %) in Victorian (Irving, 1974) and other New South Wales examples (Binns *et al.*, 1970). Very low Cr probably reflects the relatively low Cr concentrations in the host melts (85–106 ppm) and also the preferential entry of Cr into coexisting clinopyroxenes (Seward, 1971). Compared with clinopyroxene megacrysts from a variety of alkaline hosts in New South Wales (Binns *et al.*, 1970) and Victoria (Irving, 1974), the Nandewar examples generally have lower Al and Na and higher Ca.

Ca-rich pyroxene phenocrysts are more generally less abundant than olivine phenocrysts in the hawaiites and they are subordinate to plagioclase and anorthoclase phenocrysts in trachyandesites and trachytes, respectively. Ca-rich groundmass pyroxenes decrease in abundance over the compositional range trachyandesite–trachyte and in the comendites and peralkaline trachytes their place is taken by Na-rich pyroxenes.

TABLE I. *Olivine analyses*

	Hawaiite & Trachyandesites					Tristanites		Trachytes		
Sample No.[1]	49000	49001	49008	49009	49012	49076	49081	49088	49103	49085
	PC	MPC	PC	MPC	MPC	PC	MPC	MPC	MPC	MPC
SiO_2	39.31	39.12	38.45	36.11	34.88	35.42	33.51	31.27	30.58	30.03
FeO*	17.29	17.82	19.14	32.87	40.67	36.85	47.13	58.79	60.16	62.90
MnO	0.17	0.18	0.10	0.61	0.98	0.75	1.27	2.36	2.68	2.49
NiO	0.24	0.33	0.29	0.21	–	–	–	–	–	–
MgO	42.73	41.94	41.60	28.76	22.90	26.31	17.50	6.89	5.11	3.83
CaO	0.23	0.38	0.24	0.58	0.57	0.33	0.43	0.65	0.61	0.52
Total	99.97	99.77	99.82	99.14	100.00	99.66	99.84	99.96	99.14	99.77
mg[2]	81.5	80.7	79.5	60.9	50.1	56.0	39.8	17.3	13.1	9.8

* Total Fe as FeO   PC – Phenocryst core   MPC – Microphenocryst core

[1] Sample numbers refer to specimens in the collection at the Department of Geology and Geophysics, University of New England.

[2] *mg* = 100 Mg/(Mg+Fe)

TABLE II. *Pyroxene analyses*

Sample No.	Hawaiites & Trachyandesites											
	49000		49001		49008			49009			49012	
	PC	G	PC	G	MC	MC	G	MC	MC	G	PC	G
SiO$_2$	48.47	50.93	47.30	50.68	51.45	49.21	47.94	51.76	49.14	50.90	49.09	50.18
TiO$_2$	1.84	1.34	2.45	1.57	0.64	1.36	3.71	0.47	1.43	0.81	1.79	1.67
Al$_2$O$_3$	5.18	2.47	6.76	2.27	5.27	7.73	4.29	4.27	6.47	1.37	4.66	2.65
Cr$_2$O$_3$	0.41	–	0.30	–	–	0.18	–	–	–	–	–	–
Fe$_2$O$_3$*	2.51	1.96	3.04	1.32	0.59	1.15	1.00	2.19	4.36	1.71	2.51	0.99
FeO	5.49	7.18	4.91	7.66	14.76	6.71	9.87	13.49	5.29	13.28	7.05	9.61
MnO	–	–	–	0.19	0.19	–	0.23	0.19	0.19	0.57	0.25	0.31
MgO	14.03	14.19	13.54	14.16	25.39	15.21	11.36	26.28	15.12	11.10	14.15	12.84
CaO	21.41	21.62	21.56	21.50	1.49	18.49	21.49	1.41	17.70	20.16	19.92	21.08
Na$_2$O	0.37	0.42	0.46	0.35	–	0.56	0.66	–	1.11	0.46	0.48	0.37
Total	99.70	100.12	100.31	99.70	99.78	100.60	100.55	100.05	100.61	100.36	99.85	99.70
Ca	47.4	46.0	48.8	45.5	3.1	41.2	47.8	2.8	41.3	43.9	44.2	45.4
Mg	43.2	42.0	42.6	41.8	72.2	41.2	35.1	72.9	49.1	33.6	43.6	38.5
Fe^{2+}	9.4	12.0	8.6	12.7	24.7	11.6	17.1	24.3	9.6	22.5	12.2	16.1

Sample No.	Tristanite		Mafic Trachytes			Peralkaline Trachytes					Comendite	
	49076		49083	49088		49103	49161	49098		49104	49108	49163
	MPC	G	MPC	MPC	G	MPC	MPC	G	G	G	G	G
SiO$_2$	50.33	47.00	49.93	50.69	48.34	49.36	47.94	49.29	50.63	49.82	51.69	50.16
ZrO$_2$	–	–	–	–	–	–	0.21	–	–	0.32	2.34	1.68
TiO$_2$	1.18	2.45	1.31	0.59	0.60	0.64	0.47	1.07	1.43	0.32	1.71	3.04
Al$_2$O$_3$	2.95	5.03	3.36	1.20	0.89	0.98	0.77	0.64	0.56	0.89	0.65	2.73
Fe$_2$O$_3$*	2.40	2.86	2.48	1.64	2.75	1.54	1.76	11.15	18.70	31.34	29.72	25.31
FeO	9.02	11.15	7.92	15.59	22.97	20.34	24.40	19.40	12.31	4.56	–	2.69
MnO	0.30	0.38	0.25	0.69	0.90	0.70	1.12	0.84	0.45	0.74	0.31	0.20
MgO	13.09	10.60	13.10	9.30	4.12	5.72	2.51	0.35	–	–	–	0.16
CaO	20.34	20.16	21.49	20.60	18.68	20.75	19.88	13.28	7.80	0.55	0.41	1.09
Na$_2$O	0.55	0.47	0.40	0.41	0.99	0.50	0.58	4.77	8.43	11.87	13.29	12.24
Total	100.16	100.10	100.24	100.71	100.24	100.53	99.64	100.80	100.31	100.41	100.12	99.18
Ca	44.6	46.2	46.8	45.1	44.1	46.5	46.9	45.9	44.8	13.4	0.0	0.0
Mg	40.0	33.8	39.7	28.3	13.5	17.9	8.2	1.7	0.0	0.0	0.0	35.8
Fe^{2+}	15.4	20.0	13.5	26.6	42.4	35.6	44.9	52.4	55.2	86.6	100.0	64.2
Mg	67.0	57.3	69.2	48.2	21.8	31.2	14.2	2.0	0.0	0.0	0.0	0.9
Fe^{2+}+Mn	29.3	39.4	28.1	49.0	71.4	65.2	81.6	63.4	39.5	17.9	1.0	9.2
Na	3.7	3.3	2.7	2.8	6.8	3.6	4.2	34.6	60.5	82.1	99.0	89.9

* Calculated following Papike et al. (1974)

PC – phenocryst core   MC – megacryst core   MPC – microphenocryst core   G – groundmass

The compositional trend on the pyroxene quadrilateral (fig. 3) is comparable with that displayed by other mildly alkaline suites from Oki Dogo (Uchimizu, 1966), Canobolas Volcano, New South Wales (Middlemost, 1981) and south-east Queensland (Ewart, 1981) but differs from the Boina and Erta Ale pyroxene trends (Bizouard *et al.*, 1980) in its essentially constant Ca content (except for the megacrysts) over a wide range of Fe/Mg ratios.

Al contents of clinopyroxene megacrysts typically are higher than those of low-pressure Ca-rich pyroxenes although some groundmass Ca-rich pyroxenes have Al contents comparable with those in megacrysts. However, groundmass pyroxene Al is dominantly in tetrahedral coordination, whereas much of the Al in the megacrysts is in octahedral coordination, as the Ca-Tschermak's component CaAl$_2$SiO$_6$ (Kushiro, 1962). Wass (1979) noted similar variability in total Al contents of coexisting megacryst and groundmass pyroxenes in basaltic

rocks from the southern highlands of New South Wales and the Massif Central, France.

Decreasing pyroxene M values [i.e. $M = 100\ Mg/(Mg + Fe^2)$ with Fe^{3+} calculated following Papike et al. (1974)] correlate with decreasing host and increasing pyroxene Mn content, the latter reaching a maximum of 1.40 wt. % MnO in ferrohedenbergite phenocrysts in several comendites. Mn contents of clinopyroxenes are consistently lower than in coexisting olivines indicating preferential partitioning of Mn into olivine.
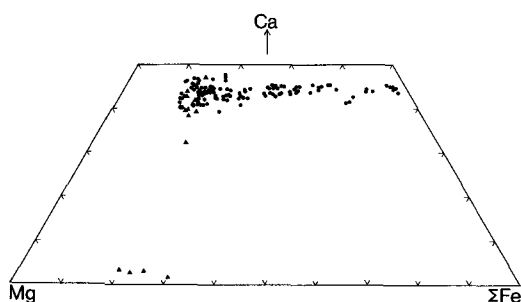

FIG. 3. Analyses of Ca-rich and Ca-poor pyroxenes plotted in terms of atom percent Ca, Mg, and ΣFe ($Fe^{2+} + Fe^{3+} + Mn$). Megacrysts (triangles) and Ca-rich phenocryst and groundmass pyroxenes (dots).

In general the Ti contents of phenocrysts and Ca-rich groundmass pyroxenes are higher than in coexisting pyroxene megacrysts. When Al^{iv} is plotted against Ti, phenocrysts and groundmass pyroxenes tend to conform to the ratio $2Al^{iv}$: Ti, suggesting the substitution of the hypothetical titanopyroxene component, $Ca\ TiAl_2O_6$ (Yagi and Onuma, 1967).

Na substitution is very limited in the compositional range augite–ferrohedenbergite except in the clinopyroxene megacrysts (e.g. Table II, No. 49009) where a small but significant $NaAlSi_2O_6$ component is indicated. Extensive solid solution between hedenbergite and aegirine in the groundmass pyroxenes from the peralkaline trachytes and comendites is illustrated in a ternary plot of acmite, diopside, and hedenbergite (fig. 4). This trend is comparable to those of other mildly alkaline volcanic series, including Oki Dogo, Japan (Uchimizu, 1966) and the Canobolas Province, New South Wales (Middlemost, 1981), as well as the undersaturated nepheline syenites of the Ilimaussaq intrusion, Greenland (Larsen, 1976). In a comparison of pyroxene crystallization trends from a variety of alkaline associations Larsen (1976) showed that there is considerable variation in the

stage of Fe^{2+} enrichment in pyroxenes at which significant substitution of Na occurs. To some extent this is evident within single specimens from the Nandewar suite as illustrated by the different trends of Na-enrichment in fig. 4.

Increases in pyroxene Fe^{3+} and Na coincide with decreases in Mn, confirming the coherence of Mn with Fe^{2+} in members of the diopside-hedenbergite series (cf. Tyler and King, 1967; Nicholls and Carmichael, 1969). Zr enrichment in passing from hedenbergite (0.2 wt. % ZrO_2) to aegirine (max. 2.3 wt. %) is comparable with that displayed by analogous pyroxenes from the Ilimaussaq intrusion (Larsen, 1976), but is substantially less than in pyroxenes from the Motzfeldt centre, south Greenland (Jones and Peckett, 1980), where aegirines with up to 7.0 wt. % ZrO_2 were considered to confirm the existence of a Zr-pyroxene end-member $[Na(Mg,Fe)_{0.5}Zr_{0.5}Si_2O_6]$.

The Ti contents of Nandewar pyroxenes close to the acmite–hedenbergite join are variable but generally increase from hedenbergite to aegirine, attaining a maximum of 3.5 wt. % TiO_2. Substitution of Ti in aegirine is accompanied by increases in Zr, Na, and possibly Mg and Mn, and by a decrease in Fe^{3+}. The preferred model for Ti (and Zr) substitution in aegirines involves solid solution between $NaFe^{3+}Si_2O_6$ and a neptunite end-member $(R^+R_{0.5}^{2+}R_{0.5}^{4+}Si_2O_6, \quad R^+ = Na \pm Ca \pm K \pm Li, \quad R^{2+} = Fe^{2+},Mg,Mn \pm Zn, \quad R^{4+} = Ti,Zr)$ proposed by Pedersen et al. (1975) and Ferguson (1977). Alternative models involving substitutions of the form $NaTi(AlSi)O_6$ and $NaTi(Fe^{3+}Si)O_6$ (Flower, 1974) do not maintain a charge balance for pyroxenes with relatively high Ti contents where there is nearly complete occupancy of tetrahedral sites by Si.

Amphiboles. Sodic-calcic and sodic amphiboles occur in the groundmass of Nandewar volcanics extending from trachyandesite to comendite. Representative analyses of amphiboles (Table III), classified following Leake (1978), range in composition from edenite (trachyandesite) and richterite-ferrorichterite (mafic trachytes) to arfvedsonite and less commonly alumino- and ferri-katophorite (peralkaline trachytes and comendites). Although amphibole was not observed in the tristanites, it is relatively abundant as reaction rims on augite in a small monzonite body which is probably the intrusive equivalent of the tristanites.

Increasing Na contents with corresponding decreases in Ca and Al in the transition from edenite to arfvedsonite are clearly illustrated in fig. 5. A ternary plot of Na–Mg–Ca (fig. 6), regarded by Larsen (1976) as analogous to the Ac–Di–Hd plot for pyroxenes (Ca $\simeq Fe^{2+}$ + Mn for Mg-poor Ca-rich pyroxenes), indicates a trend of amphibole
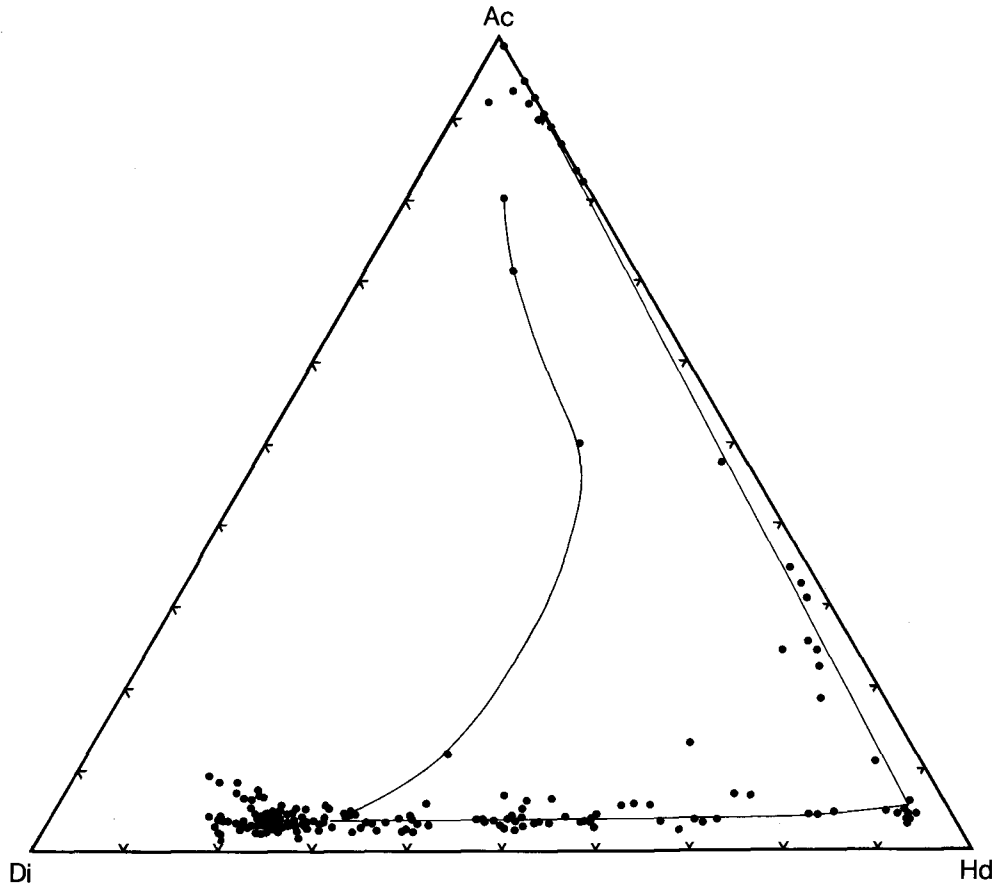
FIG. 4. Analyses of Ca-rich and Na-rich pyroxenes plotted in terms of mole percent acmite, diopside and hedenbergite. Different trends of pyroxene Na-enrichment for the suite are shown.

TABLE III *Amphibole analyses*

Sample No.	Trachyandesite 49009	Monzonite 49070	Mafic Trachytes					Peralkaline Trachytes		Comendite 49163
			49082	49082	49085	49088	49088	49100	49101	
	E	F-E	R	F-R	F-R	K	A	A	A-K	A
SiO$_2$	46.57	46.18	50.22	51.04	49.55	45.40	48.18	49.32	47.52	50.46
TiO$_2$	1.24	1.08	1.95	2.17	1.91	3.05	2.68	0.23	0.68	1.08
Al$_2$O$_3$	6.72	5.36	1.27	1.14	1.28	6.10	1.68	0.58	12.45	0.76
FeO*	16.07	21.49	18.11	21.43	27.66	30.27	32.57	34.66	25.09	34.38
MnO	0.36	0.47	0.48	0.41	0.65	0.62	0.76	1.23	0.55	0.82
MgO	13.12	10.07	11.30	8.98	4.88	1.27	1.05	0.32	0.20	–
CaO	9.87	10.02	6.11	5.38	5.48	4.25	3.62	2.99	4.83	0.96
Na$_2$O	3.31	2.22	5.74	6.09	5.98	5.90	6.55	7.47	5.64	8.85
K$_2$O	1.04	1.04	1.20	1.35	1.41	1.37	1.48	1.40	0.85	1.40
Total	98.30	97.93	96.38	97.99	98.80	98.23	98.57	98.20	97.81	98.71
mg^1	59.3	45.5	52.7	42.8	23.9	7.0	5.4	1.6	1.4	–

* Total Fe as FeO   E   Edenite   K   Katophorite   R   Richterite   A   Arfvedsonite

^1mg = 100 Mg/(Mg+Fe)   F-E   Ferro-edenite   A-K   Alumino-katophorite   F-R   Ferro-richterite

compositions which differs from the pyroxene trend (cf. fig. 4). The most notable difference is the consistently high Mg content of the amphiboles at a given Na/Ca ratio.
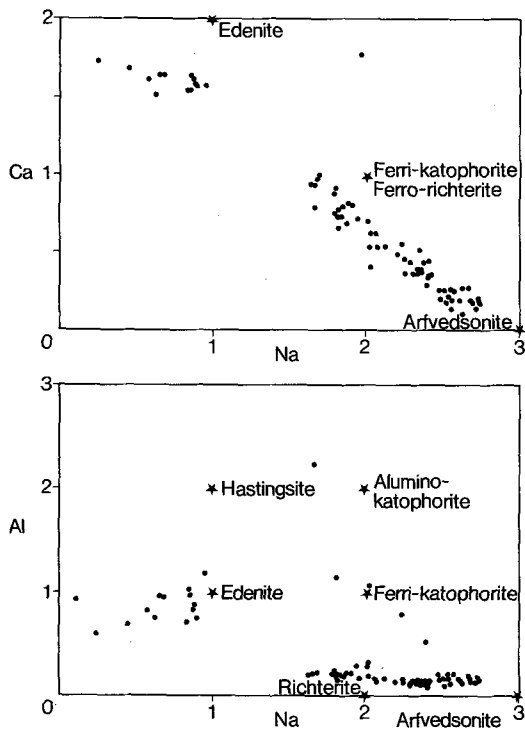

FIG. 5. Variation of Ca and Al with Na in Nandewar amphiboles showing the positions of the various end-member species.

In general the Mn contents of amphiboles increase in the transition from edenite to arfvedsonite and amphiboles coexisting with ferrohedenbergite have comparable or marginally lower Mn contents than the coexisting pyroxenes. However, the Mn content of amphibole is considerably higher than that of coexisting Na-rich pyroxene.

Fe–Ti oxides. Titanomagnetite is the dominant Fe–Ti oxide phase throughout the Nandewar suite. Ilmenite occurs occasionally as a groundmass phase and rarely it is a microphenocryst in hawaiites, trachyandesites, tristanites, and trachytes. Representative analyses of homogeneous titanomagnetites and ilmenites are given in Table IV. Throughout the suite the titanomagnetites display a considerable range in their ulvöspinel contents, the highest Fe_2TiO_4 values occurring in spinels from comendites and tristanites. However, there is

no consistent correlation between titanomagnetite Fe_2TiO_4 content and host composition because ulvöspinel contents of titanomagnetites from several comendites are comparable with those from hawaiites and trachyandesites.
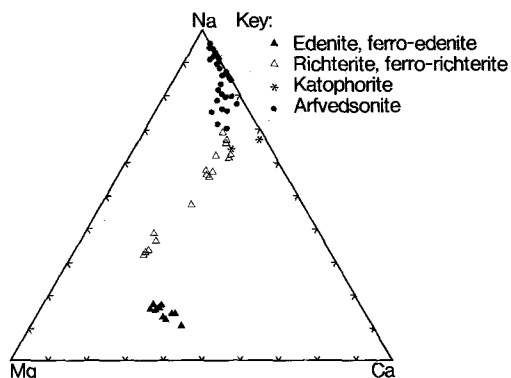

FIG. 6. Analyses of amphiboles plotted in terms of atom percent Na, Mg, and Ca.

Titanomagnetite and ilmenite phenocrysts display negligible zoning. Nevertheless groundmass titanomagnetites are usually enriched in the Fe_2TiO_4 component relative to associated phenocrysts. Prevot and Mergoil (1973) observed a similar relationship in alkali basalts from St Clement, France, whereas Wass (1973) noted the reverse trend in alkali basalts and basanites from southern New South Wales. Increased Fe_2TiO_4 content of groundmass spinels is probably due to decreases in oxygen fugacities and Fe^{3+}/Fe^{2+} ratios (and hence increased Fe_2TiO_4) in the residual liquids as a result of cooling and early precipitation of titanomagnetite.

Titanomagnetite phenocrysts in some trachyandesites (e.g. Table IV, No. 49010) may be moderate pressure cognate precipitates since they are similar in composition to Fe–Ti oxides from rare inclusions rich in tschermakitic subcalcic pyroxenes. These phenocrysts are characterized by higher MgO, Al_2O_3, Cr_2O_3, and V_2O_3 than the groundmass spinels. Similar MgO and Al_2O_3 contents in spinels have been reported from Japanese trachyandesites (Aoki, 1966) and New South Wales basalts (Wass, 1973), the latter being interpreted as possible moderate pressure precipitates from their hosts.

Where titanomagnetite and ilmenite coexist, Al, Cr, and V are concentrated in the spinel phase whereas Mg is usually higher in the rhombohedral phase, presumably as the geikielite component

TABLE IV. *Analyses of titanomagnetite, ilmenite and aenigmatite*

Titanomagnetite

Sample No.	Hawaiites & Trachyandesites						Tristanite	Mafic Trachytes		Peralkaline Trachyte	Comendite
	49000	49002	49003	49010	49012	49013	49076	49083	49097	49102	49161
	G	G	G	MC	MPC	G	MPC	MPC	MPC	MPC	MPC
TiO_2	24.85	24.58	23.26	13.03	21.37	27.51	24.89	23.13	28.08	22.86	23.44
Al_2O_3	1.42	1.86	1.46	6.08	3.98	1.91	2.08	1.29	1.42	0.15	0.31
V_2O_3	0.35	0.53	0.37	0.59	0.53	0.13	0.23	-	0.33	-	-
Cr_2O_3	0.17	0.51	-	0.95	-	0.14	-	-	0.17	-	-
Fe_2O_3*	20.06	18.83	23.47	37.00	24.69	14.86	18.74	23.19	13.58	24.08	23.42
FeO	50.22	49.61	49.81	38.43	46.79	52.20	50.92	50.97	55.77	50.90	50.19
MnO	0.52	0.37	0.87	0.47	0.45	0.87	0.79	0.76	0.53	1.02	1.40
MgO	2.27	2.52	1.48	3.47	3.00	2.55	1.71	0.67	0.87	-	0.14
ZnO	-	-	-	-	-	-	-	-	-	-	1.25
Total	99.86	98.81	100.72	100.02	100.81	100.17	99.36	100.01	100.75	99.01	100.15
Mol.%Usp.[1]	69.7	70.4	65.5	35.6	60.9	77.1	71.3	65.9	80.1	64.7	66.6

Ilmenite | | | | | | | Aenigmatite

Sample No.	Hawaiites & Trachyandesites				Mafic Trachyte	Peralkaline Trachyte	Peralkaline Trachytes		
	49000	49002	49003	49013	49097	49100	49098	49099	49103
	G	G	G	G	G	MPC	G	G	G
SiO_2	-	-	-	-	-	-	40.20	41.87	39.39
TiO_2	51.57	51.06	49.58	51.78	51.18	51.46	7.40	7.42	8.57
Al_2O_3	-	0.09	0.27	0.18	0.34	-	0.72	0.91	1.11
V_2O_3	-	0.32	0.23	-	-	-	-	-	-
Cr_2O_3	-	0.15	-	-	-	-	-	-	-
Fe_2O_3*	5.90	4.24	6.44	4.16	3.99	2.99	7.19	4.88	6.86
FeO	39.43	39.74	41.61	40.20	42.40	44.07	35.17	35.10	35.11
MnO	0.57	0.64	0.70	0.84	1.92	2.17	1.20	1.09	0.81
MgO	3.49	3.10	1.01	3.09	0.94	-	0.17	0.18	0.26
CaO	-	-	-	-	-	-	0.21	0.28	0.65
Na_2O	-	-	-	-	-	-	7.38	7.82	7.34
K_2O	-	-	-	-	-	-	0.10	0.15	0.12
Total	100.96	99.34	99.84	100.25	100.77	100.69	99.74	99.70	100.22
Mol.% Hm.[1]	6.3	4.6	6.5	4.4	4.1	3.0			
T°C	1020	970	990	1030	1080	-			
$-log_{10} fO_2$	11.0	12.0	11.5	11.0	10.3	-			

*   Calculated assuming stoichiometry

[1]   Calculated using the method of Carmichael (1967)

T and fO_2 estimated following Buddington and Lindsley (1964)

MPC - Microphenocryst core composition
MC - megacryst core composition
G - groundmass phase

($MgTiO_3$). Mn appears to be approximately equally distributed between coexisting titanomagnetite and ilmenite and it increases in the titanomagnetites with increasing SiO_2 content of the host, reaching a maximum of 3.5 wt. % MnO in the groundmass phase of a peralkaline trachyte. Zn was only determined on selected samples but appears to be a significant component of spinels in comendites (see Table IV, No. 49161).

Aenigmatite of restricted compositional varia-tion (Table IV) occurs as a groundmass phase in peralkaline trachytes and comendites and it occa-sionally rims titanomagnetite and ilmenite micro-phenocrysts. TiO_2 displays the most marked variation (7.33–8.57 wt. %) in the aenigmatites although variation in TiO_2 does not appear to be correlated with variation in Fe_2O_3 (calculated assuming stoichiometry, 20 anions and 14 cations) involving substitutions of the type which charac-terize aenigmatites from nepheline syenites of the

Trans Pecos province, Texas (Hodges and Barker, 1973) and the Ilimaussaq intrusion, south Greenland (Larsen, 1976). Additional substitutions of the type $CaAl \rightleftharpoons NaSi$ (Larsen, 1976) are also minimal, probably due to the very low Ca contents of the oversaturated peralkaline hosts.

Feldspars. Plagioclase is a subordinate phenocryst phase to olivine in the hawaiites but dominant over olivine and clinopyroxene in the trachyandesites and tristanites. Plagioclase phenocrysts typically exhibit normal zoning, but reverse-zoned examples do occur in several trachyandesites. Feldspar analyses (Table V) for specific rock groups have been plotted in terms of mole percent Ab, An, Or (fig. 7). Anorthoclase and sanidine from the peralkaline trachytes, comendites, and alkali rhyolites exhibit only a relatively restricted compositional range (Or_{26-49}), with a concentration of analyses

between Or_{34} and Or_{42}. This corresponds to the range of feldspar compositions broadly defining the minimum in the Ab–Or series (Tuttle and Bowen, 1958).

Systematic differences exist between the Or contents of phenocryst and groundmass alkali feldspars in the mafic trachytes and peralkaline rocks. Phenocrysts in the former group generally are zoned from Ab-rich cores to more Or-rich rims, a trend extended by groundmass feldspar compositions. The peralkaline rock types generally exhibit the reverse trend, with relatively Or-rich phenocryst cores and more Ab-rich rims and groundmass compositions. The data for the peralkaline rocks contrast with that of Nicholls and Carmichael (1969) for peralkaline salic lavas from Pantelleria and New Zealand, where the compositional zoning is in the opposite sense (i.e. relatively Ab-rich cores

Table V. *Feldspar analyses*

Sample No.	Hawaiites & Trachyandesites										Tristanites		
	49000	49001	49008		49011		49012		49076			49081
	PC	MPC	PC	G	PC	G	G	G	PC	G		PC
SiO$_2$	52.84	54.69	57.83	55.22	54.23	60.33	63.78	65.48	56.28	64.72		59.26
Al$_2$O$_3$	29.82	28.12	26.24	27.21	28.68	24.71	21.82	19.95	27.24	21.63		25.21
Fe$_2$O$_3$*	0.34	0.56	0.27	0.79	0.64	0.89	0.42	0.46	0.57	0.56		0.44
CaO	12.38	10.66	8.01	9.96	11.02	6.24	2.98	0.93	9.54	2.12		6.86
Na$_2$O	4.18	5.15	6.56	5.75	5.14	7.51	7.40	5.87	5.82	7.86		6.84
K$_2$O	0.37	0.50	0.77	0.54	0.43	0.79	3.53	7.86	0.60	3.65		1.12
Total	99.93	99.68	99.68	99.47	100.14	100.47	99.93	100.55	100.05	100.54		99.73
Ab	37.1	45.3	57.1	49.5	44.6	65.5	65.1	50.8	50.7	68.8		60.2
An	60.7	51.8	38.5	47.4	52.9	30.0	14.5	4.4	45.9	10.2		33.3
Or	2.2	2.9	4.4	3.1	2.5	4.5	20.4	44.8	3.4	21.0		6.5

Sample No.	Mafic Trachytes				Peralkaline Trachyte		Comendites			Alkali Rhyolites	
	49083		49088		49098		49161	49164		49121	49130
	MPC	MPC	PC	PR	PC	G	PC	PC	G	PC	PC
SiO$_2$	61.09	62.96	63.61	65.51	66.04	66.56	66.13	66.33	66.31	65.86	66.33
Al$_2$O$_3$	24.25	22.69	21.63	19.46	19.61	19.48	19.60	19.25	19.72	19.49	19.03
Fe$_2$O$_3$*	0.38	0.44	0.38	0.46	0.21	0.58	0.17	–	0.17	0.13	0.18
BaO	–	–	1.78	0.46	–	–	–	–	–	–	–
CaO	5.42	2.81	2.20	0.43	0.40	0.39	0.26	0.19	0.45	0.48	–
Na$_2$O	7.41	7.19	6.92	6.75	6.46	7.33	7.44	7.26	8.48	6.56	7.31
K$_2$O	1.47	4.16	4.37	6.38	7.61	5.80	6.29	6.85	4.74	7.04	6.45
Total	100.02	100.25	100.89	99.45	100.33	100.14	99.89	99.88	99.87	99.56	99.30
Ab	65.2	62.6	60.9	59.8	52.3	64.5	63.5	61.1	71.6	57.3	63.2
An	26.3	13.5	10.7	2.1	1.9	1.9	1.2	0.9	2.1	2.3	–
Or	8.5	23.9	28.8	38.1	42.8	33.6	35.3	38.0	26.3	40.4	36.8

* Total Fe as Fe$_2$O$_3$; PC – Phenocryst core; PR – Phenocryst rim; MPC – Microphenocryst core;
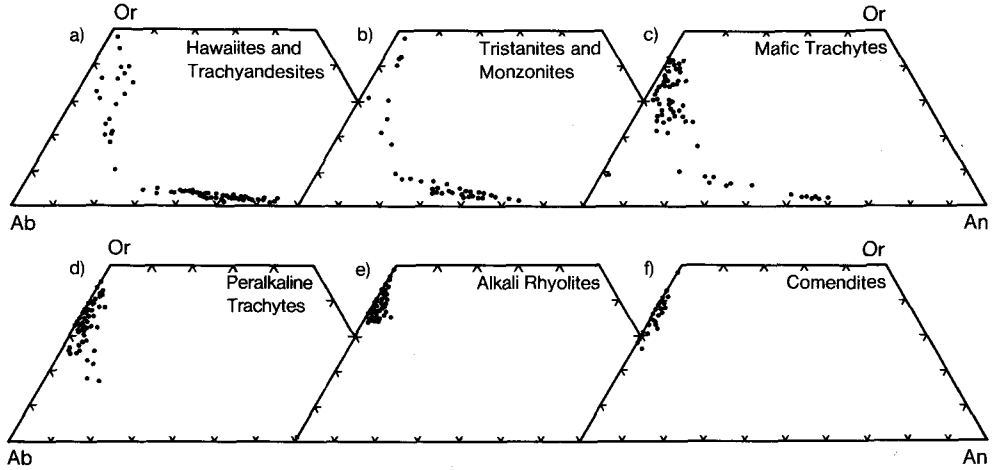
G – Groundmass composition.

FIG. 7. Feldspar analyses plotted in terms of mole percent Ab, Or, and An.

to Or-rich rims). However, the data on the Nandewar feldspars are consistent with the conclusion of Bailey and Schairer (1964), that in general feldspars are more potassic than the liquids from which they separate. Bailey and Schairer (1964) termed this the 'orthoclase effect' because the separation of such feldspars fractionates K_2O and Al_2O_3 from peralkaline liquids.

Although variable, the Fe content of the alkali feldspars is usually a little lower than that of plagioclases. Fe generally concentrates in groundmass phases and phenocryst rims relative to phenocryst cores for plagioclase and alkali feldspar from all rock types (Fig. 8). Bizouard et al. (1980) observed a similar relationship in plagioclases from Boina and Erta Ale lavas and suggested this reflects an increase in f_{O_2} (and Fe^{3+}/Fe^{2+}) in the liquids at the effusive stage. This interpretation is inconsistent with increased Fe_2TiO_4 contents in Nandewar groundmass spinels compared with associated phenocrysts. In general, Fe substitution in alkali and plagioclase feldspars increases with crystallization temperature and increased An content in plagioclase (Smith, 1975). Higher Fe contents in
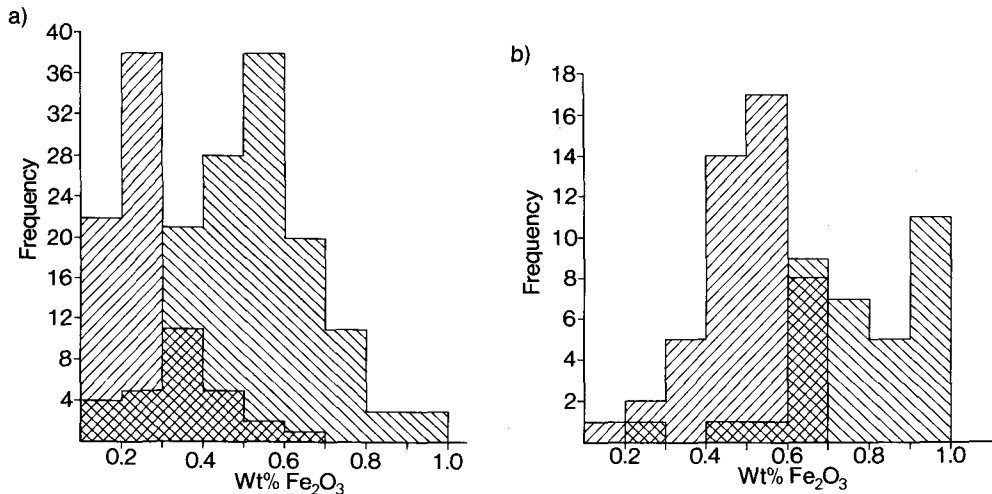

FIG. 8. Frequency histograms of Fe_2O_3 content (wt. %) in phenocryst cores (positive slope diagonals) and groundmass (negative slope diagonals) (a) alkali feldspars and (b) plagioclase feldspars.

groundmass feldspars relative to associated pheno-
crysts cannot therefore be attributed to tempera-
ture or such simple compositional controls because
they would be expected to produce the opposite
trend. A possible explanation is that the Fe con-
tents of feldspars are governed by rate of crystalliza-
tion (Brown and Carmichael, 1971). Disorder in
feldspars increases with temperature (Stewart,
1975) and more rapid rates of cooling and crystal-
lization (Martin, 1974). Disordering would there-
fore be more pronounced in rapidly crystallized
groundmass feldspars and phenocryst rims. If sub-
stitution of Fe for Al is enhanced by disordering, as
is suggested by Mossbauer studies on lunar plagio-
clases (Hafner, 1975), there would be more potential
for Fe substitution into relatively more disordered
groundmass feldspars.

Reverse-zoned plagioclase phenocrysts coexist-
ing with aluminous clinopyroxene and ortho-
pyroxene megacrysts may also represent moderate-
pressure precipitates. Plagioclase megacrysts have
been recognized in both alkaline and tholeiitic
hosts from a number of localities (e.g. Nigeria—
Wright, 1968; Japan—Aoki, 1970; New Mexico—
Hoffer and Hoffer, 1973; New South Wales—
Duggan and Wilkinson, 1973; California—Laughlin
et al., 1974). The more Ab-rich nature of plagioclase
megacrysts relative to the low pressure rims and
coexisting phenocrysts is most easily explained by
rapid transfer of the megacrysts from a relatively
high to lower pressure regimes. Experimental
studies on basaltic and andesitic melts (Cohen
et al., 1967; Thompson, 1972) indicate that under
moderately dry conditions, liquidus or near-
liquidus plagioclases exhibit systematic increases in
Ab content with increasing pressure.

Petrological implications

$T-P-f_{O_2}$ conditions during crystallization. Crys-
tallization temperatures of the Nandewar volcanics,
based on the compositions of coexisting clino- and
orthopyroxene megacrysts (Wood and Banno,
1973; Wells, 1977), pyroxene/melt equilibria
(Nielsen and Drake, 1979), coexisting Fe–Ti oxides
(Buddington and Lindsley, 1964; Spencer and
Lindsley, 1981) and plagioclase/liquid data (Kudo
and Weill, 1970; Mathez, 1973), are summarized in
fig. 9. Application of the two-pyroxene geothermo-
meter is not strictly justified for coexisting ortho-
pyroxene and clinopyroxene megacrysts in the
trachyandesites because the two phases may not
have been in equilibrium. However, temperatures
calculated by the method of Wells (1977) are in
close agreement with those calculated using the
plagioclase/liquid geothermometer for $P_{H_2O} = 0.5$ to
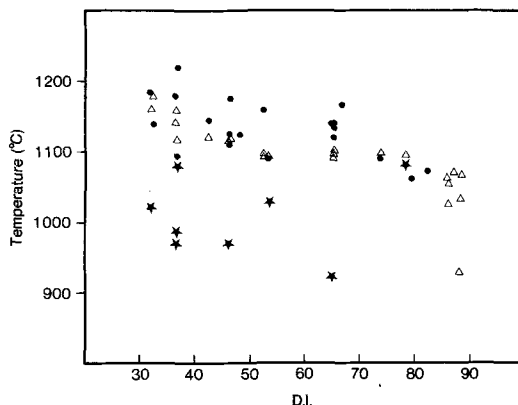1.0 kbar. Temperatures calculated using coexisting

FIG. 9. Summary of geothermometric data in a plot of
calculated temperature versus differentiation index (DI) of
the host. The various temperatures were calculated using
plagioclase (dots), pyroxene (triangles) and Fe–Ti oxide
(asterisks) compositional data.

Fe–Ti oxide data (Table IV) are significantly lower
than those calculated by other methods. This is
probably because the Fe–Ti oxides were principally
groundmass phases and hence provide quench
temperatures. Temperatures obtained from the
calibration of Buddington and Lindsley (1964) were
consistently 100–200 °C higher than those derived
from the curves of Spencer and Lindsley (1981). The
former appear more consistent with other calcu-
lated and experimental data and are thus preferred.

The megacryst assemblages in the trachyande-
sites are regarded as liquidus or near-liquidus
phases, and by analogy with the experimental data
of Knutson and Green (1975) on a hawaiite from
New South Wales, the Nandewar pyroxene mega-
crysts probably precipitated from their hosts at
temperatures of 1100–1150 °C.

Calculated near-liquidus and quench tempera-
tures decrease with increasing DI (differentiation
index) of the host (fig. 9) and are in the range
1000–1100 °C for the mafic trachytes based on
pyroxene/liquid and plagioclase/liquid data for
$P_{H_2O} = 0.5–1.0$ kbar. The peralkaline trachytes
and rhyolites presumably crystallized at somewhat
lower temperatures (cf. Bizouard et al., 1980) but
unfortunately available mineralogical data do not
permit temperature estimates for these rocks.

The presence of aluminous mildly subcalcic
pyroxenes and aluminous bronzites in several
trachyandesite flows indicates a period of crystal-
lization for their hosts at elevated pressures. Ex-
perimental studies on melts of similar composition
from the Comboyne Province, New South Wales
(Knutson and Green, 1975), and Auckland Island,

New Zealand (Green and Hibberson, 1970), indicate that orthopyroxene is a near-liquidus phase at 6.5 and 15 kbar, respectively, in melts, containing approximately 2 wt. % H_2O. The megacryst-bearing Nandewar volcanics and megacryst compositions most closely resemble the 6–8 kbar experimental data of Knutson and Green (1975). The Auckland Island host (Green and Hibberson, 1970) is more magnesian ($M = 66$) than the megacryst-bearing Nandewar trachyandesites ($M = 50$) and it contains megacrysts which are more aluminous and subcalcic than the Nandewar examples. These are inferred from experimental data to have crystallized at 14–16 kbar.

None of the other Nandewar eruptives contains any mineralogical evidence of crystallization at elevated pressures and thus are inferred to have only experienced intratelluric crystallization in a relatively low-pressure (< 5 kbar) environment.

Where possible oxygen fugacities (Table IV) have been estimated from coexisting Fe–Ti oxide pairs (Buddington and Lindsley, 1964; Spencer and Lindsley, 1981). As with estimates of temperature, the f_{O_2} estimates based on the latter calibration are consistently lower, by 0.5–3.8 orders of magnitude. In view of the apparently imprecise nature of these estimates it is probably desirable to discuss only general trends in the T–f_{O_2} data, although the values derived from the curves of Buddington and Lindsley (1964) can be directly compared with previous estimates for alkaline rocks. These data (e.g. Anderson, 1968; Prevot and Mergoil, 1973; Wass, 1973; Bizouard et al., 1980) and also those for many tholeiitic volcanics (e.g. Carmichael, 1967; Anderson and Wright, 1972; Thompson, 1975) cluster about the synthetic FMQ buffer curve when T is plotted against f_{O_2} and they exhibit a trend of decreasing f_{O_2} with decreasing T. A similar plot for the Nandewar data (fig. 10) indicates a similar trend with most points plotting parallel to and just below the synthetic FMQ buffer curve. The presence of ilmenite microphenocrysts with a very low R_2O_3 content (3.0 mole percent Fe_2O_3) and the assemblage fayalite–titanomagnetite–quartz (the natural analogue of the synthetic FMQ buffer) in some of the peralkaline trachytes indicates extension of this trend to lower T and f_{O_2} conditions. Experimental data on the stability relations of alkali amphiboles (Ernst, 1962; Charles, 1975, 1977) and aenigmatite (Ernst, 1962; Lindsley, 1971) which occur in the peralkaline trachytes and comendites further support the contention that these lavas crystallized under relatively low f_{O_2} conditions between the MW and NNO buffers.

Close correspondence of the trend in fig. 10 to the synthetic buffer curves supports the proposal of Carmichael and Nicholls (1967) that magmas are
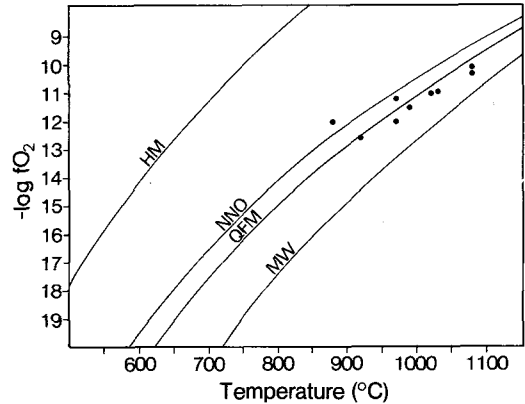

FIG. 10. Plot of $-\log f_{O_2}$ versus temperature for coexisting Fe–Ti oxide pairs. The synthetic buffer curves have been reproduced from Buddington and Lindsley (1964) for comparison.

'internally buffered' for at least part of their cooling history. The available T–f_{O_2} data for the Nandewar suite can be interpreted as indicating that temperature was the dominant control on f_{O_2} (Wass, 1973) and changes in melt Fe^{3+}/Fe^{2+} and O^{2-} resulting from fractionation of solid phases apparently were minimal.

The voluminous older rhyolites uniformly display extensive alteration of ferromagnesian silicates and original titanomagnetite, indicative of pervasive late-stage oxidation of those eruptives and a higher f_{O_2} in the melt during crystallization compared with the comendites which contain groundmass arfvedsonite and aenigmatite.

Stability of Na-rich pyroxenes, amphiboles, and aenigmatite. In synthetic systems acmite is stable under very low oxygen fugacities, in equilibrium with a fayalite–magnetite–quartz (FMQ) assemblage and iron metal, respectively (Bailey, 1969; Gilbert, 1969). However, in natural assemblages aegirine does not necessarily appear to crystallize under such highly reduced conditions. in pantellerites from Pantelleria (Carmichael, 1962; Nicholls and Carmichael, 1969) and Ethiopia (Bizouard et al., 1980) the pyroxene phenocrysts interpreted to have crystallized under f_{O_2} conditions equal to or slightly less than those defined by the FMQ buffer, are sodic ferrohedenbergites. Olivine is absent from Nandewar rocks which contain aegirine, and in rocks where titanomagnetite or ilmenite occur as microphenocrysts, these phases are rimmed by aenigmatite. This suggests that in the natural systems, crystallization of aegirine occurs under oxygen fugacities not controlled by the FMQ buffer

and also supports the concept of a 'no-oxide' field in T-f_{O_2} space for silicic volcanics in which acmite coexists with aenigmatite and Fe–Ti oxides are absent (Nicholls and Carmichael, 1969). Nash and Wilkinson (1970) noted that the appearance of Na-rich pyroxenes in the Shonkin Sag intrusion coincided with the disappearance of olivine and relatively enhanced f_{O_2} of the magma subsequently buffered by the assemblage annite–magnetite–alkali-feldspar.

Although the stability of aegirine is clearly sensitive to fluctuations in f_{O_2}, it is difficult to estimate the relative importance of controls such as liquid composition, T and f_{O_2} on the development of the four major mafic groundmass assemblages in the Nandewar peralkaline rhyolites and trachytes. These assemblages are: (1) Na-rich pyroxene + aenigmatite + arfvedsonite; (2) aegirine + arfvedsonite; (3) aenigmatite + arfvedsonite; (4) arfvedsonite.

The coexistence of Na-rich pyroxenes with aenigmatite and arfvedsonite [the latter two phases are considered to be unstable at oxygen fugacities significantly greater than those of the FMQ buffer (Bailey, 1969; Lindsley, 1971)] suggests that liquid composition may also be important in controlling the stability of these assemblages. For example, Bailey (1969) concluded that acmite only crystallizes from liquids containing excess Na_2SiO_3, given that T and f_{O_2} are appropriate. Increases in the Fe^{3+}/Fe^{2+} ratio of the liquids accompany increases in alkali content (Paul and Douglas, 1965; Carmichael and Nicholls, 1967; Kogarko, 1974) and the resultant increase in the Na/Fe^{2+} ratio of the liquid, may assist in stabilizing aegirine together with arfvedsonite and aenigmatite under oxygen fugacity conditions which are possibly not the most favourable for the crystallization of aegirine alone. Lower Na/Fe^{2+} ratios and high P_{F_2} and P_{H_2O} conditions would favour the precipitation of arfvedsonite (Ernst, 1968). The effect of high P_{F_2}, a common attribute of peralkaline acid liquids (Kogarko, 1974), is to decrease the oxygen fugacity. The coexistence of aegirine and arfvedsonite (devoid of a reaction relationship) in the groundmass of peralkaline lavas supports the suggestion of Nash and Wilkinson (1970) that they are stable over a narrow T-f_{O_2} compositional range.

The occurrence of groundmass Na-rich pyroxenes which extend into vesicles in a metaluminous trachyte suggests a different control on their formation. The mode of occurrence together with evidence of late-magmatic oxidation effects suggest that these Na-rich pyroxenes precipitated from a Na, Fe and H_2O-rich fluid phase during degassing of the lava. The absence of coexisting F-rich amphiboles, which do occur in the vesicles of peralkaline rocks, indicates that P_{F_2} was low and

the f_{O_2} was relatively high compared with the peralkaline lavas. Oxidation may have occurred as a result of selective hydrogen loss in a gaseous phase following dissociation of H_2O (Sato, 1978).

Experimental data on the stability relations of richterite–ferrorichterite solid solutions (Charles, 1975, 1977), indicate that their maximum temperature stability is strongly dependent on composition and oxygen fugacity. The Mg end-member (richterite) is stable to 1030 °C at 1 kbar P_{total} for a wide range of oxygen fugacities. However, ferrorichterite on the IW buffer is stable to only 715 °C at 1 kbar P_{total}, and with increasing oxygen fugacity the maximum temperature stability of ferrorichterite decreases (525 °C at 1 kbar and the FMQ buffer). These data indicate that the Nandewar ferrorichterites precipitated at temperatures between approximately 650 and 750 °C under low to moderate oxygen fugacities (probably between the MW and FMQ buffers).
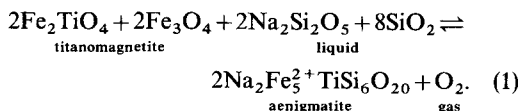
Charles (1975) suggested that the appearance of richterite was favoured by melts characterized by normative qz and metasilicate, high volatile content, and low f_{O_2} for iron-rich varieties. The general restriction of richterite and ferrorichterite to mafic trachytes of the Nandewar suite contrasts with the dominance of arfvedsonite in moderately peralkaline lavas, whereas the peralkaline varieties may have ferrorichterite coexisting with arfvedsonite or katophorite. This apparent host rock control on the paragenesis of these phases probably reflects decreasing melt Ca contents in passing from mafic to peralkaline trachytes.

Experimental studies on the stability of riebeckite–arfvedsonite solid solutions (Ernst, 1962, 1968) indicate that arfvedsonite is stable to lower temperatures than ferrorichterite, although the high-temperature stability limit of the former is extended in the presence of a F-rich volatile phase. Ernst (1962) determined that riebeckite–arfvedsonite is stable up to 655 °C at 250 bars P_{fluid} and 712 °C at 2000 bars P_{fluid} with oxygen fugacities defined by the IW buffer.
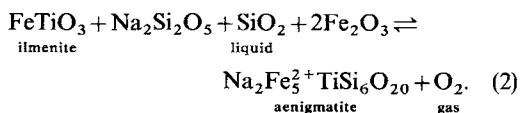
Investigation of Ti-free aenigmatite (Ernst, 1962) indicated it is stable at very low oxygen fugacities appropriate to the iron-wustite (IW) and magnetite-wustite (MW) buffers. Subsequent experimental data on 'ideal' aenigmatite (Lindsley, 1971) indicated that it is stable in the range 400–900 °C and at low to moderate oxygen fugacities. At 750 °C and 500 bars the stability curve for aenigmatite lies between the nickel–nickel-oxide (NNO) and FMQ buffer curves.

A relatively high Ti melt content was suggested by Abbott (1967) and Borley (1976) as an important factor controlling the stability of aenigmatite. Although the influence of Ti on the composition of

aenigmatite is clear from the data of Hodges and Barker (1973), low Ti concentrations in the melt apparently do not inhibit its crystallization. Instead, temperature, oxygen fugacity and $Na_2Si_2O_5$ content of the melt appear to be the most important variables controlling aenigmatite stability. Aenigmatite overgrowths on titanomagnetite microphenocrysts, also noted by Abbott (1967), Marsh (1975) and Larsen (1977), suggest a reaction of the type proposed by Marsh (1975):

$$2Fe_2TiO_4 + 2Fe_3O_4 + 2Na_2Si_2O_5 + 8SiO_2 \rightleftharpoons$$
$$\underset{\text{titanomagnetite}}{} \qquad \underset{\text{liquid}}{}$$

$$2Na_2Fe_5^{2+}TiSi_6O_{20} + O_2. \quad (1)$$
$$\underset{\text{aenigmatite}}{} \qquad \underset{\text{gas}}{}$$

Aenigmatite rimming ilmenite also suggests a reaction relationship between ilmenite microphenocrysts and residual peralkaline liquid, according to the reaction:

$$FeTiO_3 + Na_2Si_2O_5 + SiO_2 + 2Fe_2O_3 \rightleftharpoons$$
$$\underset{\text{ilmenite}}{} \qquad \underset{\text{liquid}}{}$$

$$Na_2Fe_5^{2+}TiSi_6O_{20} + O_2. \quad (2)$$
$$\underset{\text{aenigmatite}}{} \qquad \underset{\text{gas}}{}$$

Additional evidence in favour of reaction (2) is provided by the selective replacement by aenigmatite of ilmenite lamellae in titanomagnetites from pegmatoids in the Picture Gorge Basalt, Washington (Lindsley et al., 1971).

Conclusions

Olivine, pyroxene, amphibole, and feldspar compositions vary systematically and continuously throughout the suite as functions of host-rock compositions. Tschermakitic subcalcic pyroxene and aluminous bronzite phenocrysts (and perhaps some titanomagnetite and plagioclase phenocrysts) in several trachyandesites are considered to have crystallized from their hosts at approximately 6–8 kbar. The remaining volcanics display no evidence of crystallization at elevated pressures. Fe–Ti oxide data indicate generally that magmas spanning the compositional range trachyandesite–comendite crystallized under conditions of decreasing T and f_{O_2} which broadly coincided with the FMQ synthetic buffer curve. The voluminous older rhyolites differ from the trachyandesite–comendite spectrum because they appear to have suffered pervasive oxidation during eruption, possibly as a result of selective loss of H_2 following dissociation of H_2O. Crystallization of Na-rich pyroxenes in the groundmasses of some trachytes and comendites appears to have occurred over a relatively broad range of f_{O_2} conditions. Relatively low f_{O_2} conditions appear to favour coprecipitation of arfvedsonite ± aenigmatite, whereas higher f_{O_2} conditions appear to favour crystallization of Na-rich pyroxene only. Aenigmatite rims on titanomagnetite and ilmenite microphenocrysts in several peralkaline eruptives provides some support for the existence of a 'no-oxide' field in T–f_{O_2} space.

REFERENCES

Abbott, M. J. (1967) *Am. Mineral.* **52**, 1895–901.
——(1969) *Contrib. Mineral. Petrol.* **20**, 115–34.
Anderson, A. T. (1968) *Am. J. Sci.* **266**, 704–27.
——and Wright, T. L. (1972) *Am. Mineral.* **57**, 170–87.
Aoki, K. (1966) Ibid. **51**, 1799–805.
——(1970) *Contrib. Mineral. Petrol.* **25**, 284–8.
Bailey, D. K. (1969) *Am. J. Sci.* **267A**, 1–16.
——and Schairer, J. F. (1964) Ibid. **262**, 1198–206.
Binns, R. A., Duggan, M. B., and Wilkinson, J. F. G. (1970) Ibid. **269**, 132–68.
Bizouard, H., Barberi, F., and Varet, J. (1980) *J. Petrol.* **21**, 401–36.
Borley, G. D. (1976) *Mineral. Mag.* **40**, 595–8.
Brown, F. H., and Carmichael, I. S. E. (1971) *Lithos,* **4**, 305–23.
Buddington, A. F., and Lindsley, D. H. (1964) *J. Petrol.* **5**, 310–57.
Carmichael, I. S. E. (1962) *Mineral. Mag.* **33**, 86–113.
——(1967) *Contrib. Mineral. Petrol.* **14**, 36–64.
——and Nicholls, J. (1967) *J. Geophys. Res.* **72**, 4665–87.
Charles, R. W. (1975) *Am. Mineral.* **60**, 367–74.
——(1977) *Am. J. Sci.* **277**, 594–625.
Cohen, L. H., Ito, K., and Kennedy, G. C. (1967) Ibid. **265**, 475–518.
Duggan, M. B., and Wilkinson, J. F. G. (1973) *Contrib. Mineral. Petrol.* **39**, 267–76.
Ernst, W. G. (1962) *J. Geol.* **70**, 689–736.
——(1968) *Amphiboles,* Springer, New York.
Ewart, A. (1981) *J. Geophys. Res.* **86**, 10242–56.
Ferguson, A. K. (1977) *Contrib. Mineral. Petrol.* **60**, 247–53.
Flower, M. F. J. (1974) *Am. Mineral.* **59**, 536–48.
Gilbert, M. C. (1969) *Am. J. Sci.* **267A**, 145–59.
Green, D. H., and Hibberson, W. O. (1970) *Phys. Earth Planet. Inter.* **3**, 247–54.
Hafner, S. S. (1975) In *Mossbauer Spectroscopy. Topics in Applied Physics*, 5 (U. Gonser, ed.), Springer, Berlin, 167–99.
Hodges, F. N., and Barker, D. S. (1973) *Carnegie Inst. Wash. Yearb.* **72**, 578–81.
Hoffer, J. M., and Hoffer, R. L. (1973) *Geol. Soc. Am. Bull.* **84**, 2139–42.
Irving, A. J. (1974) Ibid. **85**, 1503–14.
Jones, A. P., and Peckett, A. (1980) *Contrib. Mineral. Petrol.* **75**, 251–5.
Knutson, J., and Green, T. H. (1975) Ibid. **52**, 121–32.
Kogarko, L. N. (1974) In *The Alkaline Rocks* (H. Sorensen, ed.), Wiley, New York, 474–87.

Kudo, A. M., and Weill, D. F. (1970) *Contrib. Mineral. Petrol.* **25,** 52–65.

Kushiro, I. (1962) *Jap. J. Geol. Geog.* **33,** 213–20.

Larsen, L. M. (1976) *J. Petrol.* **17,** 258–90.

——(1977) *Lithos,* **10,** 257–70.

Laughlin, W., Manzer, K. Jr., and Carden, R. (1974) *Geol. Soc. Am. Bull.* **85,** 413–16.

Leake, B. E. (1978) *Can. Mineral.* **16,** 501–20.

Lindsley, D. H. (1971) *Carnegie Inst. Wash. Yearb.* **69,** 188–90.

——Smith, D., and Haggerty, S. E. (1971) Ibid. **69,** 264–90.

Marsh, J. S. (1975) *Contrib. Mineral. Petrol.* **50,** 135–44.

Martin, R. F. (1974) In *The Feldspars* (W. S. MacKenzie and J. Zussman, eds.), Manchester University Press, Manchester, 313–36.

Mathez, E. A. (1973) *Contrib. Mineral. Petrol.* **41,** 61–72.

Middlemost, E. A. K. (1981) *Geol. Soc. Aust. J.* **28,** 33–49.

Nash, W. P., and Wilkinson, J. F. G. (1970) *Contrib. Mineral. Petrol.* **25,** 241–69.

Nicholls, J., and Carmichael, I. S. E. (1969) Ibid. **20,** 268–94.

Nielsen, R. L., and Drake, M. J. (1979) *Geochim. Cosmochim. Acta,* **43,** 1259–72.

Papike, J. J., Cameron, K. L., and Baldwin, K. (1974) *Geol. Soc. Am. Abst. Programs,* **6,** 1053–4.

Paul, A., and Douglas, R. W. (1965) *Phys. Chem. Glasses,* **6,** 207–11.

Pedersen, A. K., Engell, J., and Ronsbo, J. G. (1975) *Lithos,* **8,** 255–68.

Prevot, M., and Mergoil, J. (1973) *Mineral. Mag.* **39,** 474–81.

Roeder, P. L. (1974) *Earth Planet. Sci. Lett.* **23,** 397–410.

Sato, M. (1978) *Geophys. Res. Lett.* **5,** 447–9.

Seward, T. M. (1971) *Chem. Geol.* **7,** 73–95.

Simkin, T., and Smith, J. V. (1970) *J. Geol.* **78,** 304–25.

Smith, J. V. (1975) In *Feldspar Mineralogy. Mineral. Soc. Am. Short Course Notes* (P. H. Ribbe, ed.), **2,** SM18–29.

Spencer, K. J., and Lindsley, D. H. (1981) *Am. Mineral.* **66,** 1189–201.

Stewart, D. B. (1975) In *Feldspar Mineralogy. Mineral. Soc. Am., Short Course Notes* (P. H. Ribbe, ed.), **2,** ST1–52.

Stipp, J. J., and McDougall, I. (1968) *Austral. J. Sci.* **31,** 84–5.

Stolz, A. J. (1985) *J. Petrol.* **26,** 1002–26.

Stormer, J. C. Jr. (1973) *Geochim. Cosmochim. Acta,* **37,** 1815–21.

Takahashi, E. (1978) Ibid. **42,** 1829–44.

Thompson, R. N. (1972) *Am. J. Sci.* **272,** 901–32.

——(1975) Ibid. **275,** 1049–72.

Tuttle, O. F., and Bowen, N. L. (1958) *Geol. Soc. Am., Mem.* 74.

Tyler, R. C., and King, B. C. (1967) *Mineral. Mag.* **36,** 5–21.

Uchimizu, M. (1966) *J. Fac. Sci. Univ. Tokyo, Sec. II,* **16,** 85–159.

Ware, N. G. (1981) *Comput. Geosci.* **7,** 167–84.

Wass, S. Y. (1973) *Geol. Soc. Aust. J.* **20,** 427–48.

——(1979) *Lithos,* **12,** 115–32.

Watson, E. B. (1979) *Am. Mineral.* **64,** 824–9.

Wellman, P., and McDougall, I. (1974) *Geol. Soc. Aust. J.* **21,** 247–72.

——McElhinny, M. W., and McDougall, I. (1969) *R. Astron. Soc., Geophys. J.* **18,** 371–95.

Wells, P. R. (1977) *Contrib. Mineral. Petrol.* **62,** 129–39.

Wilkinson, J. F. G., and Stolz, A. J. (1983) Ibid. **83,** 363–74.

Wood, B. J., and Banno, S. (1973) Ibid. **42,** 109–24.

Wright, J. B. (1968) *Nature,* **218,** 262–3.

Yagi, K., and Onuma, K. (1967) *J. Fac. Sci. Hokkaido Univ.* **13,** 463–83.